Indian Journal of Fibre & Textile Research
Vol. 50, December 2025, pp. 463-470
DOI: 10.56042/ijftr.v50i4.14154

Controlled synthesis and performance study of hard elastic polypropylene fibres

Yuanyuan Li, Yantao Gao[a], Wenfeng Hu & Zan Lu

School of Textiles and Fashion, Shanghai University of Engineering Science, Shanghai 201 620, China

Received 20 October 2024; revised received and accepted 17 July 2025

This study explores the fabrication process and performance characterisation of hard elastic polypropylene (PP) fibres. The fibres have been produced through melt spinning, followed by controlled stretching and post-processing treatments. Their structural and functional properties are examined using scanning electron microscopy (SEM), thermogravimetric analysis, differential scanning calorimetry, synchrotron radiation computed tomography, and mechanical testing. The results demonstrate that the fibres exhibit remarkable hard-elastic behaviour. Clear differences appear in the stress-strain curves between room temperature and water bath stretching. This variation is attributed to the possible formation of sub-crystalline structures during water-bath stretching, while slow cooling in air promotes structural optimisation and improved crystallisation. Furthermore, fibres extruded at 240 °C and subsequently annealed at 140 °C demonstrate the highest levels of elastic recovery and crystallinity, confirming the importance of precise thermal control in achieving superior mechanical performance.

Keywords: Controlled fabrication, Elastic recovery, Hard elasticity, Melt spinning, Polypropylene fibres

1 Introduction

With the rapid advancement of materials science, high-performance fibre materials continue to demonstrate significant potential across diverse sectors, including textiles, healthcare, construction, automotive engineering, and aerospace. Among these materials, polypropylene (PP) is widely recognised for its versatility as a thermoplastic, owing to its chemical resistance, thermal stability, electrical insulation, high mechanical strength, and excellent abrasion resistance. In addition, PP is readily recyclable, enabling the utilisation of reclaimed or discarded PP during production[1]. As a result, PP fibres and related materials are extensively employed in apparel, blankets, concrete reinforcements, medical devices, automotive components, bicycles, conveyor pipes, chemical containers, lithium battery separators, and capacitor dielectric films[2-7]. Nevertheless, conventional PP fibres exhibit notable limitations, particularly in elastic recovery, wear resistance, and fatigue resistance, which restrict their suitability for certain high-end technical applications.

Hard-elastic polypropylene, as a representative of hard-elastic materials, has garnered increasing attention due to its distinctive hard-elastic behaviour. Its notable feature is the ability to maintain a high modulus while exhibiting excellent elastic recovery. This characteristic is primarily attributed to its unique processing method, which facilitates the formation of a lamellar crystalline structure oriented perpendicular to the stress direction, along with well-structured amorphous regions. Typically, the degree of hard elasticity of the material is assessed by measuring the elastic recovery rate after stretching.

Previous research highlights the advantageous mechanical behaviour of hard-elastic PP fibres. Quynn reported that stretching induces the separation of crystalline lamellae, leading to the formation of microvoids within the fibre structure[8]. These features, together with the fibres' high elasticity, make them suitable for impact-resistant protective fabrics and medical elastic bandages, while also imparting lightweight and breathable characteristics. Sprague[9] observed that, in contrast to conventional fibres, the diameter of hard-elastic fibres remained nearly unchanged during stretching. This stability, combined with the formation of micropores and the intrinsic chemical resistance of PP, enables applications in filtration media and in chemical industry materials used for nanoparticle loading[10]. Park[11]further noted that hard-elastic behaviour is retained even at extremely low temperatures (–190 °C) when fibres are stretched in liquid nitrogen. Noether *et al.* discovered that hard-elastic materials demonstrate superior creep and stress relaxation properties, with the stress

[a]Corresponding author.
E-mail: gaoyantao@sues.edu.cn

relaxation resistance further enhanced after thermal treatment[12]. This holds potential for applications in wearable flexible fabrics and shape-memory composites. Additionally, hard-elastic materials retain their properties across various solvents[13]. Ren[14] found that solvents, such as liquid nitrogen, can induce hard-elastic behaviour in these materials.

Although several studies have investigated the unique responses of hard-elastic PP, the literature remains limited in understanding the structural evolution under varying temperature conditions, and the underlying principles and precise control of experimental conditions to achieve high-performance hard-elastic PP fibres are relatively sparse. Therefore, this study aims to explore the preparation of hard-elastic PP fibres and conduct a comprehensive investigation into the macroscopic morphology and mechanical properties of the produced fibres. The goal is to delineate the formation range of hard elasticity, thereby providing a solid foundation for the development of high-performance hard-elastic PP fibres and further elucidating the origins of hard elasticity.

2 Materials and Methods

2.1 Materials

The PP masterbatch used in the study was grade F2401, supplied by the Yanshan Branch of Sinopec Beijing. It had a melt flow index of 2.5 g/10 min. Differential scanning calorimetry (DSC) analysis revealed a melting point of 168 °C.

2.2 Preparation of Hard-Elastic PP fibres

Hard-elastic PP fibres were prepared using a single-screw extruder equipped with a 25 mm screw diameter and a 2 mm spinneret. The screw rotation speed was maintained at 18 rpm, and the spinning temperature ranged from 190°C to 260°C. The extruded fibres were cooled at room temperature(25°C). A wet spinning and winding machine (model HZ-SF-41, Qingdao Nogu Environmental Technology Co., Ltd.) with adjustable winding speed was used to collect the fibres. The fibres obtained were annealed at 120 °C, 130 °C, and 140 °C for 1 h, respectively.

The preparation process involved heating the PP pellets to a molten state. The melt was then extruded through the spinneret, followed by high-speed stretching and cooling to obtain oriented fibres. These fibres were subsequently heat-treated to produce hard-elastic fibres, as outlinedin Fig. 1.

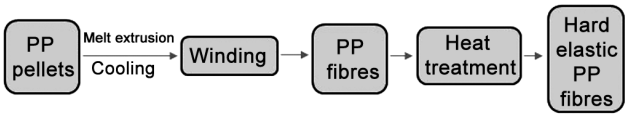

Fig. 1 — Flow chart of the hard-elastic PP fibre preparation process

2.3 Characterisationof Hard-Elastic PP Fibres

2.3.1 Elastic Recovery Rate Test

Elastic recovery rate (ER) refers to the percentage of the original length that a material can recover after being stretched to a predetermined length. Also known as the rebound rate, the elastic recovery rate is a critical indicator of a material's hardness and elasticity, reflecting its degree of elasticity. A higher elastic recovery rate indicates better lamellar alignment and superior hard-elastic properties.

Testing was conducted using an XS (08)F2 fabric strength tester (Shanghai Xusai Instrument Co., Ltd.). The clamping distance was set to 10 mm, and the stretching speed was 200 mm/min. During the experiment, the recovery rate of 10 mm fibres was recorded after being cyclically stretched to 50% of their original length five times under standard atmospheric conditions.

$$E_R = \frac{L_1 - L_2}{L_1 - L_0} \times 100\%$$

where E_R is the elastic recovery rate (%); L_0, initial length of the specimen before stretching (mm); L_1, length after stretching(mm); and L_2,length after recovery (mm).

2.3.2 Synchrotron Radiation Computed Tomography (SR-CT)

In situ measurements of the prepared hard-elastic fibres before and after stretching, as well as of the non-annealed fibres, were conducted using the BL13HB beamline at the Shanghai Synchrotron Radiation Facility (SSRF), with a resolution of 0.325 μm.

2.3.3 SEM

The cross-sections of the hard-elastic PP fibres were fixed onto a vertical test stage using conductive adhesive. The samples were then coated with a thin layer of gold and placed on a copper holder. The samples were examined under vacuum using a scanning electron microscope operated at 10 kV to observe cross-sectional morphology at high resolution.

2.3.4 DSC

Thermal behaviour was analysed using a DSC4000 (PerkinElmer Instruments, Shanghai). Samples were

heated from 30 °C to 400 °C at a rate of 10 °C/min under a nitrogen atmosphere, held isothermally for 5 min to remove thermal history, and subsequently cooled to 30 °C. The heat of fusion change curve was recorded. The degree of crystallinity (Xc) was determined by integrating the melting enthalpy area, with a value of 209 J/g for completely crystalline materials[15].

2.3.5 TGA

The thermal stability of the PP masterbatch was assessed using a TGA4000 (PerkinElmer Instruments (Shanghai) Co., Ltd.) employing a constant heating rate method. Approximately 5-8 mg of dried sample was placed in a crucible, with nitrogen as the protective gas. The temperature range was set from 30°C to 600°C, with a heating rate of 20°C/min. The purpose of this test and subsequent analysis was to provide a basis for the process parameters in the subsequent spinning process and to prevent material degradation.

3 Results and Discussion

According to the TGA results, the used masterbatch begins to exhibit a decrease in weight at approximately 352°C. During the experiment, when the temperature is set to 190°C, the melt drawn from the masterbatch exhibits discontinuities and brittleness and appears light yellow. In contrast, fibres typically obtained after melt drawing are expected to be transparent. This colour discrepancy is attributed to the incomplete melting of PP at the lower temperature, resulting in the presence of residual crystalline particles. These particles promote self-nucleation, which in turn raises the crystallisation temperature.

3.1 Effects of Melt Temperature on Fibre Properties

To examine how melt temperature influences fibre elasticity, the melt is extruded through a spinneret at temperatures of 200°C, 210°C, 220°C, 230°C, 240°C, 250°C, and 260°C. The resulting fibres are annealed at 120 °C, 130 °C, and 140 °C for 1 h each. The variation in the fibre's elastic recovery rate with respect to melt temperature is illustrated in Fig. 2.

As shown in Fig. 2, all three sets of fibres exhibit a similar trend: the elastic recovery rate increases initially, then decreases, rises again, and finally declines as the melt temperature increases. The elastic recovery rate reaches a relatively high level at 220 °C. A slight reduction occurs at 230 °C, followed by a peak around 240 °C. Above 240 °C, the recovery rate declines.

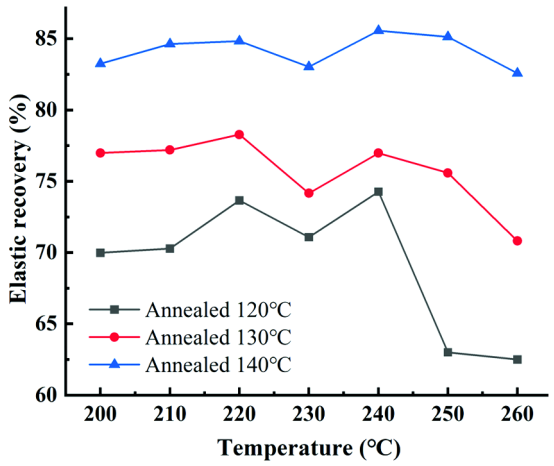

Fig. 2—Tensile curves of fibres produced at different melt temperatures

This phenomenon can be attributed to the regulatory effect of melt temperature on the material properties. At lower spinning temperatures, the melt viscosity is higher, which restricts the mobility of the molecular chains, leading to a decrease in the crystal growth rate[16]. As the temperature gradually increases to 220°C, the melt viscosity decreases, providing more energy for the molecular chains to rearrange[17]. This not only effectively enhances the orderliness of the molecular chains but also accelerates the crystal growth rate. When the fibres are subjected to external forces, stress is effectively transmitted between the crystals, while the reinforcing effect of the crystal framework is diminished[18,19]. This leads to an improvement in the fibre' selastic recovery rate. However, when the temperature increases to 230°C, the intermolecular forces weaken, which makes chain segment sliding easier. This results in an increase in plastic deformation, which consequently leads to a decrease in the elastic recovery rate. As the temperature further increases to 240°C, the fibre orientation improves, and the entanglement strength of the molecular chains is enhanced. Under external forces, the fibres can recover more effectively, leading to an increase in the elastic recovery rate once again. However, when the temperature exceeds 240°C, the crystallinity and orientation of the fibres decrease. This is because excessively high temperatures reduce the material's viscosity, making it difficult for the fibres to form during the drawing process. In addition, high temperatures may also induce material degradation, causing molecular chain

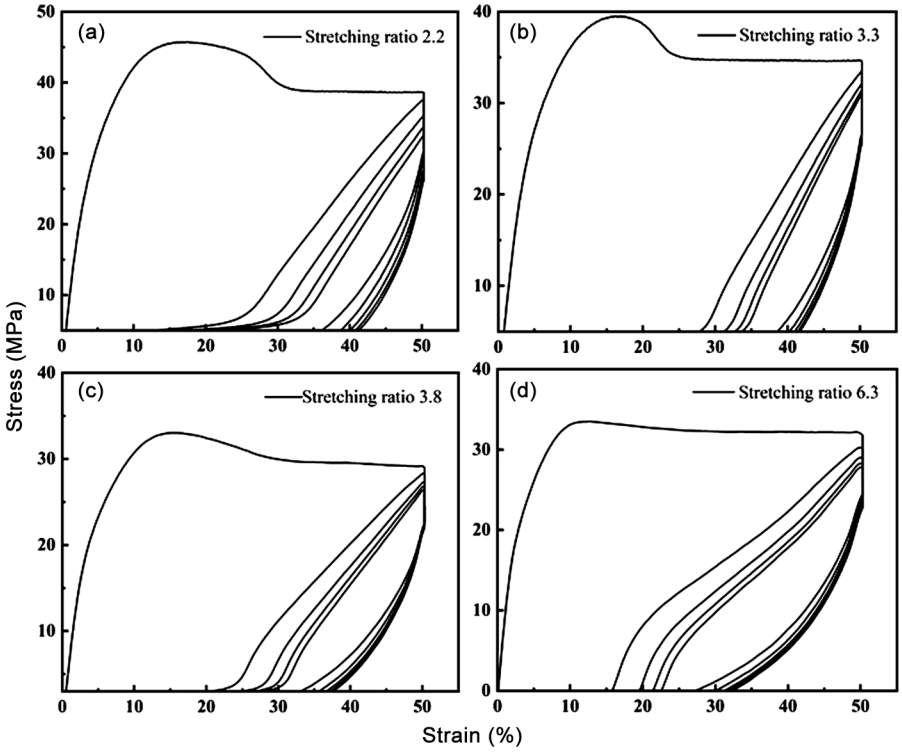

Fig. 3 — The Cyclic stress-strain curve of different draw ratios (a) 2.2, (b) 3.3, (c) 3.8 and (d) 6.3

rupture and thereby reducing the fibre's tensile resilience[20].

3.2 Impact of Stretching on Fibre Properties

Fig. 3 shows the stress-strain curves of fibreswith different draw ratiosproduced at 230 °C and annealed at 120 °C for 1 h. The curves show the characteristic response of hard-elastic materials: an initial rapid increase in stress with strain, a pronounced inflection at the point of slight deformation, and a subsequent ability of the material to recover to near its original state upon removal of the applied force after reaching the specified elongation.

During fibre stretching, a noticeable difference arises between the initial and subsequent stretching curves. Repeated stretching-recovery cycles reduce both stress levels and recovery rates, but after several cycles, the fibrestabilises. This behaviour is attributed to the disruption of the originally parallel lamellae, producing microcracks and voids[9,21,22]. When fibre under goes continuous deformation and is stretched again within a short period, the damage and defects in the crystalline structure from previous stretching donot have sufficient time to recover, exacerbating the damage with each new stretch and resulting in a continual decline in elastic recovery rate. However, with repeated stretching, the additional damage introduced by each new stretch diminishes, while the damage from previous stretches has more time to self-repair. Consequently, the elastic recovery rate of the fibre eventually approaches a relatively stable value[11]. Furthermore, providing the fibre with adequate recovery time after stretching could allow for more effective repair of the structural damage, potentially enhancing the fibre's elastic performance.

Under relatively low stretching conditions, the prepared PP samples display a distinct yield point on the stress-strain curve. At this stage, the molecular chains in the fibres have ample time to relax, but the degree of crystal orientation is relatively low, resulting in lower fibre elasticity. As the stretching ratio increases, the yield point on the stress-strain curve becomes less pronounced. The samples begin to show characteristics of hard elasticity, with the yield point disappearing[23]. With further increases in the stretching ratio, the elasticity of the fibres improves to some extent. This enhancement is attributed to the higher stretching ratio, which reduces the degree of molecular chain disorientation and improves the fibre's orientation, thereby leading to a more ordered arrangement of molecular chains and enhanced tensile recovery performance. However, excessively high

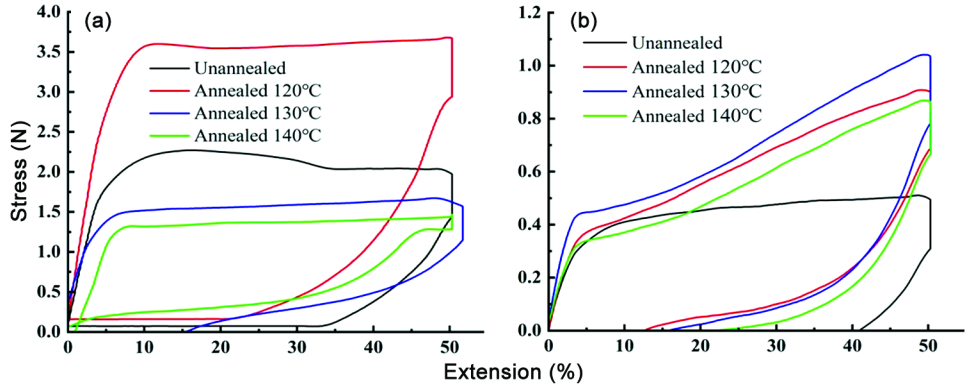

Fig. 4 — Tensile curves of fibres under different stretching conditions (a) melt drawn from the spinneret at25°C, and (b) melt drawn in a water bath

stretching ratios may also prevent molecular chains from relaxing adequately, leading to defect formation, the emergence of microcracks, and an increase in void structures, which in turn reduce the stress level. Continued stretching might cause further plastic deformation in the fibres, ultimately resulting in a decrease in elastic recovery rate.

Figure 4 compares fibres drawn from the spinneret at room temperature [Fig. 4(a)]and in a water bath[Fig. 4(b)]. A significant difference is observed between these stretching curves. In the initial stage of stretching, both tensile curves show a linear increase in fibre deformation with applied force. However, in Fig. 4(a), the curve reaches the yield point at approximately 10% deformation, after which the strength of the as-spun fibres declines until the elongation reaches 30%, at which point it stabilises. For fibres annealed at 130°C and 140°C, they elongate slowly with increasing force beyond the yield point. In contrast, the curve in Fig. 4(b) reaches the yield point at approximately 5% deformation, and the fibres continue to elongate with increasing force. Notably, for the same deformation, the fibres drawn from the water bath experience lower forces. This is due to the rapid cooling of the melt during water bath drawing, which might lead to the formation of secondary crystalline structures. Compared to the rapid cooling in the water bath, air-drawing allows for slower cooling, which is more conducive to optimising the internal structure and improving crystallisation of the fibers[24]. Therefore, fibres drawn in air exhibit higher strength.

3.3 Effect of Annealing Temperature on FibreProperties

Table 1 summarises the mechanical properties of fibres annealed at different temperatures. The

Table 1 —Structural parameters of the fibres

Annealing temp., °C	Tensile strength, MPa	Elongation at break, %
0	307.86±5.31	722.20±12.43
120	273.35±3.82	544.45±15.26
130	370.67±5.22	576.47±13.57
140	303.43±4.35	448.06±12.43

Table 2 — Effect of annealing temperature on elastic recovery of the fibres

Melting temp., °C	Elastic recovery rate, %		
	Annealing (120°C)	Annealing (130°C)	Annealing (140°C)
200	69.98	76.99	83.25
210	70.28	77.20	84.63
220	73.66	78.28	84.84
230	71.08	74.16	83.03
240	74.27	76.98	85.56
250	63.00	75.59	85.13
260	62.50	70.82	82.58

unannealed fibres show the highest elongation at break, while fibres annealed at 140 °C show the lowest. Strength is lowest at 120 °C and highest at 130 °C. This behaviour is attributed to the fact that an optimal annealing temperature can enhance the internal structure of the fibres and improve their mechanical properties.

To investigate the effect of annealing temperature on the elastic recovery rate of fibres, fibresare annealed at 120°C, 130°C, and 140 °C for 1 h each. Subsequent tensile recovery tests are performed, and the elastic recovery rates are summarised in Table 2. The data indicate that at an annealing temperature of 120°C, the elastic recovery rate ranges from 60% to 70%; at 130°C, it ranges from 70% to 80%; and at 140°C, it ranges from 80% to 86%. This demonstrates

that the elastic recovery rate of the fibres increases with the annealing temperature. At an appropriate annealing temperature, internal stresses in the fibres can be relieved, allowing the molecular chains to relax fully and transition the amorphous regions within the fibres to a crystalline state, thereby facilitating recrystallisation. Consequently, the structural uniformity of the fibres is improved, enhancing the fibre elasticity.

To contextualise performance, data from published literature and commercially available PP fibres specifications are reviewed. Currently, PP fibres are widely used in the construction industry due to their ability to effectively reduce the permeability and water absorption of concrete. Additionally, their excellent chemical resistance and superior mechanical properties significantly enhance the durability and mechanical performance of concrete[25-29]. In terms of tensile strength, commercially available PP fibres commonly used in concrete have a strength of 486MPa[30]. In studies on the modification of PP fibres with nano-calcium carbonate to improve the bonding between the fibres and the cement matrix, the fibres' tensile strength was 400 MPa[31]. In studies investigating the influence of PP fibres on the mechanical and durability properties of cement-based composites, the fibre tensile strength was 469MPa[32]. The tensile strength of PP fibres used in textiles was 562 MPa[33]. Although the tensile strength of the hard-elastic PP fibres prepared in this study is slightly lower than that of the aforementioned commercial products, their elastic recovery performance is significantly superior: under a 50% elongation with a 5-second hold in the stretched state, the recovery rate reaches 85%. In contrast, the instantaneous rebound rate of PP fibres commonly found in commercial product manuals is 88%–98% when stretched by 5%. This excellent performance, combined with other properties of PP, demonstrates a broad application potential in fields such as impact protection, intelligent sensing, and chemical product filtration.

Fig. 5(a) and (b) present the DSC curves for fibres that are not annealed, and those annealed at 120°C, 130°C, and 140°C, respectively. Further analysis of these curves yields the crystallisation parameters of the fibres, as detailed in Table 3. The melting temperatures are as follows: 167.3°C for the non-annealed fibres; 167.8 °C for fibres annealed at 120 °C; 166.5 °C for fibres annealed at 130 °C; and 169.1 °C for fibres annealed at 140°C.

As shown in the melting curves in Fig. 5(a), the non-annealed fibres exhibit a lower melting temperature, which increases with the rise in annealing temperature. When the annealing temperature reaches 140°C, the fibres exhibit the highest melting temperature. This is attributed to the fact that during the heat treatment process, an appropriate temperature effectively promotes the rearrangement of molecular chains within the fibres. The regularity of the molecular chains increases, and

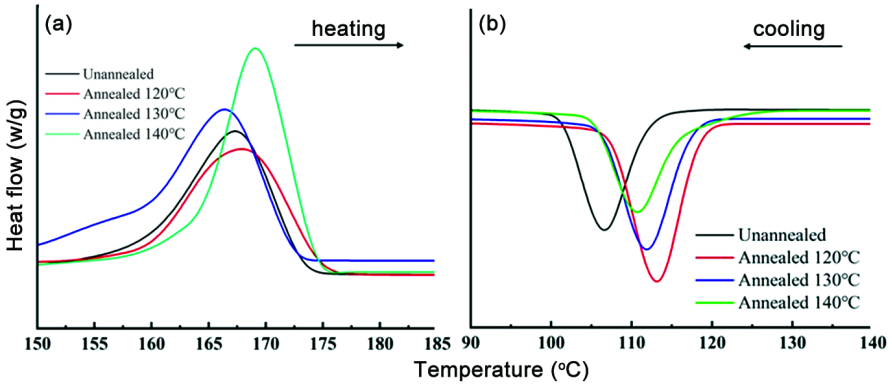

Fig. 5 — DSC curves of the fibres during (a) heating and (b) cooling

Table 3 — Crystallisation parameters of the fibres

Annealing temp., °C	Xc, %	Tc, °C	Tm, °C	Endothermic enthalpy, J/g	Exothermic enthalpy, J/g
0	28.6	106.7	167.3	59.9	60.1
120	28.0	113.1	167.8	58.6	81.1
130	30.3	111.9	166.3	67.6	67.6
140	40.1	110.7	169.0	83.9	58.0

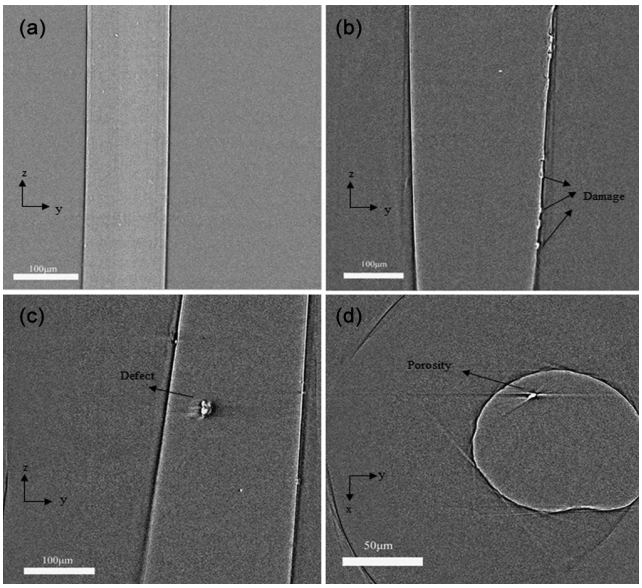

Fig. 6 — Cross-sectional and longitudinal views of fibres (a) unstretched fibre, (b) stretched fibre cross-section showing damage, (c) stretched fibre cross-section showing defects, and (d) stretched fibre cross-section showing pores

the defective regions transition into more ordered areas, leading to an increase in both the melting point and crystallinity of the fibres. This also indicates the formation of more perfect fibre crystals. As shown in the cooling curves in Fig. 5(b), the non-annealed fibres exhibit the lowest crystallisation temperature. After annealing, the crystallisation temperature of the fibres initially increases and then decreases, but remains higher than that of the non-annealed fibres. This is because annealing treatment enhances the crystallinity of the fibres, facilitates the perfection of the crystalline structure, and increases the thickness of the crystalline lamellae, thereby resulting in an elevation in the crystallisation temperature. As shown in Table 3, the crystallinity is highest at 140°C, reaching a value of up to 40%.

3.4 Surface Morphology Analysis

To investigate the surface characteristics of the hard-elastic fibres and the changes occurring before and after stretching, CT and SEM analyses are performed on the fibres.

CT images show that the fibre cross-section is circular. The unstretched fibre [Fig. 6(a)] exhibits a smooth internal structure without significant features. After stretching [Fig. 6 (b) –(d)], distinct internal damage, pores, and defects appear due to the separation of crystalline lamellae perpendicular to the fibre axis.

Figure 6(a) reveals that the internal structure of the unstretched fibre is smooth and devoid of distinctive features. In contrast, significant internal changes are observed in the stretched fibres, including the presence of pores and varying degrees of damage and defects. This phenomenon results from the separation of crystalline lamellae perpendicular to the fibre axis, leading to the formation of interconnected voids. Stress concentration around these voids causes localised damage and defects, which, to some extent, degrade the fibre's mechanical properties. Furthermore, higher stretching rates result in increased damage and defects within the fibre, causing a more pronounced adverse effect on the overall fibre performance.

SEM images of stretched fibres (Fig. 7) further confirm morphological changes. Fig. 7(a) reveals that the fibre cross-sections exhibit voids and uneven surfaces after rupture, while Fig. 7 (d) shows a significant number of voids on the fibre surface. Figs 7(c) and (d) provide a clearer view of cracks and defects on the stretched fibre surfaces, which occur around internal voids and exhibit arcuate cracks. During longitudinal deformation, crystal arrays separate and expand, creating various-sized voids and gaps between initially closely packed adjacent lamellae. When subjected to external tensile forces, the fibres turn white; upon removal of the force, they exhibit elastic recovery and become transparent. This whitening under large deformation stress demonstrates critical stress behaviour independent of stretching temperature, with the critical stress increasing with molecular weight, indicating that the mechanism is due to the breakage and relaxation of highly oriented amorphous networks (primarily straightened microfibril interchain molecules)[34].

4 Conclusion

This study systematically explores the optimisation range for the preparation of hard elastic PP fibres through precise control of melt-spinning conditions and demonstrates that controlled processing conditions play a decisive role in achieving superior hard-elastic behaviour. Experimental results indicate that melt spinning followed by stretching and appropriate thermal annealing effectively promotes the formation of oriented lamellar structures and enhances crystallinity. Fibres stretched in air exhibit higher strength than those drawn in a water bath, primarily due to slower cooling, which allows better optimisation of the internal structure. Among the tested conditions, fibres extruded at 240 °C and annealed at 140 °C achieve the highest elastic

recovery and crystallinity, confirming that both processing temperature and thermal treatment critically influence the development of hard-elastic properties. Structural analyses, including SEM, DSC, TGA, and synchrotron radiation CT, further support that the combined effects of stretching mode, cooling environment, and annealing temperature govern the macroscopic and microscopic performance of the fibres.

It is noteworthy that the trends in fibre strength and elastic recovery rate with different conditions are not entirely consistent, suggesting the potential for flexible adjustment of process parameters to achieve high-performance hard elastic PP fibres based on specific requirements. Currently, due to the limitations in cost control and performance enhancement of the available hard elastic fibre materials they remain primarily in the experimental research phase. Thus, an in-depth exploration of the material's hard elastic behaviour and its extensive applications will be a key focus for future research on hard elastic materials.

References

1 Wang X, *Plastic Sci Technol*, 38 (2010) 67.
2 Karamloo M, Afzali-Naniz O & Doostmohamadi A, *Constr Build Mater*, 250 (2020) 118856.
3 Singh M, Apata I E, Samant S, Wu W, Tawade B V, Pradhan N, Raghavan D & Karim A, *Polym Rev (Philadelphia, PA, U S)*, 62 (2022) 211.
4 Amin M, Tayeh B A & Agwa I S, *Case Stud Constr Mater*, 13 (2020) e00459.
5 Wu T, Wang K, Xiang M & Fu Q,*Chin J Chem*, 37 (2019) 1207.
6 Rytöluoto I, Gitsas A, Pasanen S & Lahti K, *Eur Polym J*, 95 (2017) 606.
7 Mehrab A H & Esfahani M R, *Period Polytech Civ Eng*, 66 (2022) 1278.
8 Quynn G R, Brody H, Sobering E S, Park K K, Foley L R, Noethe D H & Hutchison D J, *J Macromol Sci*, 4(1970) 953.
9 Sprague B, *J Macromol Sci, Part B: Physics*, 8 (1973) 157.
10 Arzhakova O, Dolgova A, Yarysheva A Y, Nikishin I & Volynskii A, *ACS Appl Polym Mater*, 2 (2020) 2338.
11 Park I & Noether H,*Colloid Polym Sci*, 253 (1975) 824.
12 Noether H & Whitney W, *Springer*, 21 (1973) 991.
13 Cannon S, Statton W & Hearle J, *Polym Eng Sci*, 15(1975) 633.
14 Ren W, *Colloid Polym Sci*, 270(1992) 943.
15 Cheng S Z, Janimak J J, Zhang A & Hsieh E T, *Polymer*, 32(1991) 648.
16 Lin H, Yan F, Guo J, Huang X, Jiang S & Xu M, *Polym Bull*, 37(2024) 358.
17 Ren Y, Li Z, Li X, Su J, Li Y, Gao Y, Zhou J, Ji C, Zhu S & Yu M, *Mater*, 17 (2024) 890.
18 Kara Y, *Springer Nature Switzerland*, (2023) 43.
19 Men Y, *Macromol*, 53 (2020) 9155.
20 Al-Zubiedy A & Muneer R M , *Prod Eng Arch*, 24 (2019) 20.
21 Quynn G R, Brody H, Sobering E S, Park K K, Foley L R, Noethe D H, Whitney W, Pritchart R, Seiminki A M, Hutchison D J, Wagner L H, Sumit J N, Sakaku K, Karneluisson R & Hutchison DJ, *J Macromol Sci*, *Part B*, 4 (1970) 953.
22 Samuels R J, *J Polym Sci: Polym Physi Edit*, 17 (1979) 535.
23 Xu G, Du Q & Wang LH, *Makromol Rapid Commun*, 8 (1987) 539.
24 Ross S E, *J Appl Polym Sci*, 9 (1965) 2729.
25 Li Y, Zhang Y, Yang E-H & Tan KH, *Cem Concr Res*, 116 (2019) 168.
26 Fallah S & Nematzadeh M,*Constr build mater*, 132 (2017) 170.
27 Cao S, Yilmaz E & Song W, *Constr Build Mater*, 223 (2019) 44.
28 Xue G, Yilmaz E, Song W & Cao S,*Compos Part B: Eng*, 172 (2019) 131.
29 Xue G, Yilmaz E, Song W & Yilmaz E, *Constr Build Mater*, 213 (2019) 275.
30 Yuan Z & Jia Y, *Constr Build Mater*, 266 (2021) 121048.
31 Feng J, Yang F & Qian S,*Constr Build Mater*, 269 (2021) 121249.
32 Li Z, Guo T, Chen Y, Fang C, Chang Y & Nie J, *J Build Eng*, 90 (2024) 109335.
33 Qin Y, Li Y, Zhang X & Zhou H, *Constr Build Mater*, 347 (2022) 128508.
34 Lu Y, Coates P & Men Y, *FEDT*, (2017) 3.